

Improving Lithium Therapeutics by Crystal Engineering of Novel Ionic Cocrystals

Adam J. Smith,^{*,†} Seol-Hee Kim,[†] Naga K. Duggirala,[§] Jingji Jin,[‡] Lukasz Wojtas,[§] Jared Ehrhart,^{||} Brian Giunta,[‡] Jun Tan,^{||} Michael J. Zaworotko,[§] and R. Douglas Shytle[†]

[†]Center of Excellence for Aging and Brain Repair, Department of Neurosurgery and Brain Repair, Morsani College of Medicine, University of South Florida, Tampa, Florida 33612, United States

[‡]Neuroimmunology Laboratory, Department of Psychiatry and Behavioral Neurosciences, Morsani College of Medicine, University of South Florida, Tampa, Florida 33612, United States

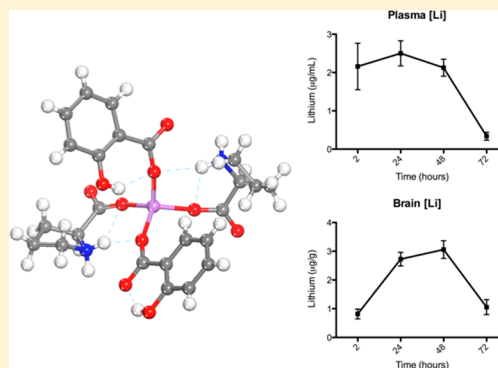
[§]Department of Chemistry, College of Arts and Sciences, University of South Florida, Tampa, Florida 33612, United States

^{||}Rashid Laboratory for Developmental Neurobiology, Silver Child Development Center, Department of Psychiatry and Behavioral Neurosciences, Morsani College of Medicine, University of South Florida, Tampa, Florida 33612, United States

S Supporting Information

ABSTRACT: Current United States Food and Drug Administration (FDA)-approved lithium salts are plagued with a narrow therapeutic window. Recent attempts to find alternative drugs have identified new chemical entities, but lithium's polypharmacological mechanisms for treating neuropsychiatric disorders are highly debated and are not yet matched. Thus, re-engineering current lithium solid forms in order to optimize performance represents a low cost and low risk approach to the desired therapeutic outcome. In this contribution, we employed a crystal engineering strategy to synthesize the first ionic cocrystals (ICCs) of lithium salts with organic anions. We are unaware of any previous studies that have assessed the biological efficacy of any ICCs, and encouragingly we found that the new speciation did not negatively affect established bioactivities of lithium. We also observed that lithium ICCs exhibit modulated pharmacokinetics compared to lithium carbonate. Indeed, the studies detailed herein represent an important advancement in a crystal engineering approach to a new generation of lithium therapeutics.

KEYWORDS: lithium, cocrystals, bipolar disorder, gsk-3, pharmacokinetics



INTRODUCTION

Lithium salts have a long history of human consumption beginning in the 1800s. In psychiatry, they have been used to treat mania and as a prophylactic for depression since the mid-20th century.¹ Today, lithium salts are used as a mood stabilizer for the treatment of bipolar disorder and also, off-label, for other psychiatric indications. For example, lithium is the only drug that consistently reduces suicidality in patients with neuropsychiatric disorders.^{2–4} Despite these effective medicinal uses, current United States Food and Drug Administration (FDA)-approved lithium pharmaceuticals (lithium carbonate and lithium citrate) are plagued with a narrow therapeutic window that requires regular monitoring of plasma lithium levels and blood chemistry by a clinician to mitigate adverse events. Still, many patients undergoing lithium therapy find the side effects to be unbearable, which negatively affects compliance and discourages physicians from utilizing lithium. These problems arise because lithium's site of action is the brain, and current lithium salts cross the blood-brain-barrier slowly.^{5,6} As a result, there is unnecessary accumulation of lithium ions in peripheral organs, particularly in the kidneys and heart, where side effects can arise. Thus, multiple

administrations throughout the day are required to safely reach therapeutic concentrations. Further, the patient must remain keenly aware of their hydration status as dehydration promotes a more rapid serum chemical imbalance with renal and cardiac toxicity. Unfortunately, the serum concentrations required to maintain therapeutic efficacy often lead to metabolic adverse effects such as hypothyroidism, hyperparathyroidism, weight gain, and nephrogenic diabetes insipidus.⁷ If supratherapeutic serum concentrations of lithium are achieved, lithium intoxication ensues. Patients with lithium poisoning can exhibit loss of consciousness, muscle tremor, epileptic seizures, and pulmonary complications.⁸ Left untreated, lithium intoxication can lead to death.

Because lithium is so effective at reducing manic episodes and suicidality in patients with bipolar disorder, it is still used clinically despite its narrow therapeutic index and serious side

Received: September 25, 2013

Revised: November 4, 2013

Accepted: November 5, 2013

Published: November 5, 2013



effects. This has motivated a search for alternatives to lithium with similar bioactivities. The problem with this approach is that the mechanism of action remains elusive. Nevertheless, recent studies have identified many important bioactivities of lithium that may be responsible for its therapeutic efficacy in its current FDA-approved indications and beyond. For example, lithium exerts neuroprotective effects, in part, by increasing brain-derived neurotrophic factor (BDNF). Chronic lithium treatment has been shown to increase the expression of BDNF in rats⁹ and humans.¹⁰ This increase in BDNF activity can lead to restoration of learning and memory deficits through promotion of neurogenesis and long-term potentiation (LTP). Another neuroprotective mechanism of lithium is attenuation of the production of inflammatory cytokines like IL-6 and nitric oxide (NO) in activated microglia.¹¹ This is particularly important since aberrant microglial function is a common finding in a number of neuropsychiatric diseases.¹² Moreover, recent lines of evidence have implicated BDNF¹³ and NO¹⁴ in novel mechanisms for lithium's antidepressant effects.

Lithium has also been found to inhibit certain enzymes in a noncompetitive manner by displacing the required divalent cation, magnesium.¹⁵ Two of these enzymes that have important implications in bipolar disorder are glycogen synthase kinase-3 beta (GSK-3 β) and inositol monophosphatase (IMPase). GSK-3 β was first identified as the molecular target of lithium by Klein and Melton.¹⁶ It functions by phosphorylating glycogen synthase, the rate-limiting enzyme of glycogen biosynthesis.¹⁷ GSK-3 β inhibitors like lithium generally produce antidepressant-like and antimania-like effects in animal models, which have been used to explain lithium's efficacy for bipolar disorder.¹⁸ GSK-3 β is expressed in all tissues, with particularly abundant levels in the brain.¹⁹ Therefore, this enzyme is thought to have tremendous potential as a therapeutic target for the treatment of a variety of neurological diseases that are characterized by dysregulated GSK-3 β such as Alzheimer's disease, HIV associated neurocognitive disorders, and autism spectrum disorders.^{20–22}

In addition to inhibiting GSK-3 β , lithium also inhibits inositol monophosphatase (IMPase) leading to cerebral inositol depletion.^{23,24} Lithium, valproic acid, and carbamazepine, which are all used for stabilization of mood, have been shown to lead to the depletion of inositol.²⁵ This has bolstered support for the inositol depletion hypothesis of lithium therapy and has highlighted this molecular target in the search for "lithium mimetics".²⁶ However, given the frequency of suicidality as a comorbidity in patients with bipolar disorder^{27,28} and that only lithium consistently reduces suicidality in these patients, it is doubtful that selective IMPase inhibitors will produce the desired clinical outcome that can be achieved with lithium. These lines of evidence imply that the antisuicidality effects of lithium are not solely attributable to IMPase inhibition/inositol depletion.

That the solid-state structure and composition of an active pharmaceutical ingredient (API) critically impacts its drug delivery performance, especially its physicochemical properties, means that materials science plays a critical role in enabling the development of bioactive molecules as drug products. In this contribution, we report that a materials science strategy based upon crystal engineering can enable improvement of the therapeutic window of lithium while retaining the bioactivities of current FDA-approved lithium solid forms. Our approach is based upon cocrystallization, which has gained the attention of both academia and industry in the past decade. Indeed, the FDA has recently released regulatory guidelines for industry on pharmaceutical cocrystals.²⁹ Almarsson and Zaworotko have

defined pharmaceutical cocrystals as "co-crystals that are formed between a molecular or ionic active pharmaceutical ingredient (API) and a co-crystal former that is a solid under ambient conditions".³⁰ Cocrystallization is of growing interest because these multicomponent materials that are based upon two or more "coformers" can be rationally designed by crystal engineering.^{31,32} Further, they represent novel solid forms of APIs that can improve the physicochemical properties (e.g., solubility and stability), improve efficacy (e.g., bioavailability), and provide a means for extending the life cycle of existing APIs.³³

Previously, we successfully used cocrystallization of two molecular coformers to improve the solubility and consequent bioavailability of the poorly soluble bioflavonoid quercetin³⁴ and to conversely lower the pharmacokinetics of the highly soluble antioxidant epigallocatechin-3-gallate, EGCG.³⁵ The molecular cocrystals of quercetin and EGCG that we studied were stabilized by hydrogen bonded supramolecular synthons, which are assumed to dissociate *in vivo* leaving therapeutically bioactive quercetin and EGCG. Ionic cocrystals (ICCs) have even more recently emerged as another class of multicomponent pharmaceutical materials (MPMs) of scientific and practical interest.^{36–40} ICCs can be defined as "MPMs formed from a salt and a molecular or ionic compound." The general formula of ICCs is therefore A^+B^-N , where A^+ is a cation, B^- is an anion, and N is neutral molecule or another salt. If one of the components of the ICC is a pharmaceutical compound then there is considerable opportunity to modulate the physicochemical and biological efficacy of the pharmaceutical compound because there are two components that can be changed. This contrasts with single component crystals of pharmaceutical compounds, which have very limited opportunities for fine-tuning of materials properties, and other MPMs such as simple salts, A^+B^- , and molecular cocrystals, AB , for which there is only variable component besides the pharmaceutical compound.

Zaworotko et al. reported ICCs of inorganic lithium salts, Li^+B^- , with a series of amino acids, zwitterionic molecules, N , by exploiting the strength of lithium carboxylate bonds.³⁹ In these ICCs, the lithium cation (API) forms coordination bonds to the amino acid coformers and the inorganic anions remain in the composition to balance charge. Given that coordination bonds are stronger than hydrogen bonds we became interested in determining if the stronger bonding would affect the *in vivo* speciation of lithium and thereby modulate its therapeutic bioactivity and pharmacokinetics. We herein describe the synthesis of two novel ICCs of organic anion salts of lithium with the amino acid coformer, proline. We assessed the blood and brain pharmacokinetics of this new speciation of lithium in rats and their therapeutic activities at several established targets of lithium therapy.

■ EXPERIMENTAL SECTION

Reagents and Materials. Lithium salicylate ($\geq 98\%$ purity), lithium hydroxide ($\geq 98\%$ purity), nicotinic acid ($\geq 98\%$ purity), and proline ($\geq 99\%$ purity) were purchased from Sigma-Aldrich Corporation (St. Louis, MO) and used as such without further purification.

Lithium Cocrystal Syntheses. *LISPRO.* Lithium salicylate ($\geq 98\%$ pure, anhydrous, used as received from Sigma Aldrich, 1 mmol) and L-proline ($\geq 99\%$ pure, used as received from Sigma Aldrich, 1 mmol) were dissolved in 2.0 mL of hot deionized water. The resulting solution was maintained on a hot plate (75–

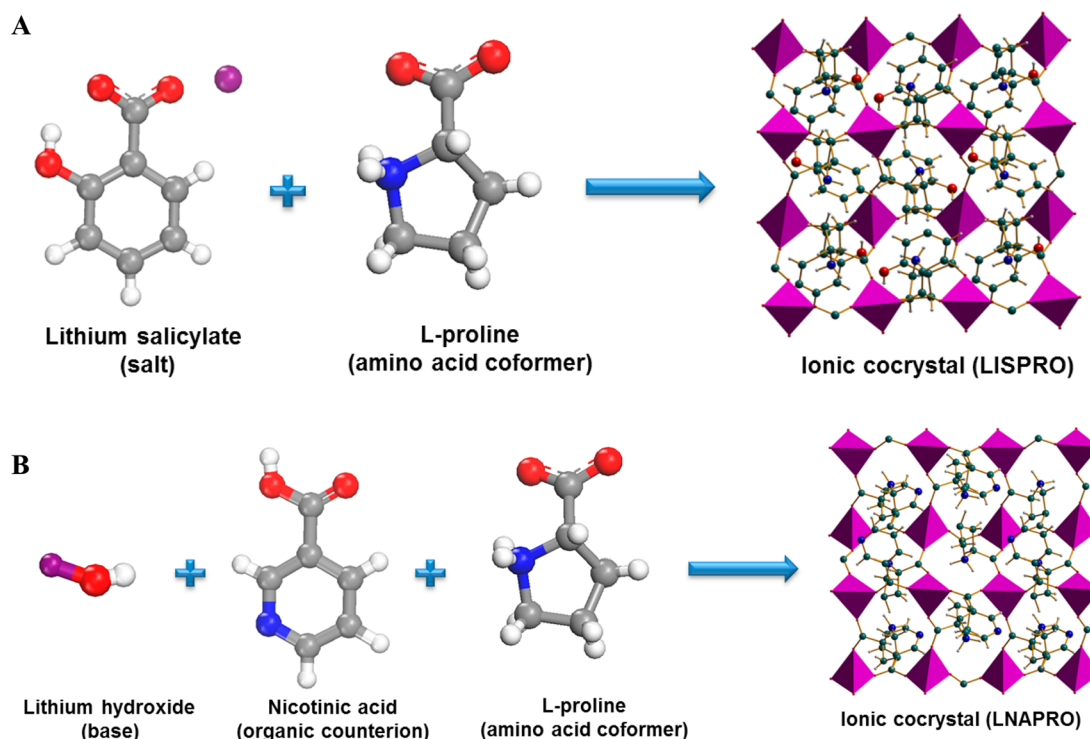


Figure 1. Reaction diagrams. Reactions for LISPRO (A) and LNAPRO (B).

90 °C) to allow slow evaporation of solvent until crystals had formed. Colorless crystals of LISPRO were collected.

LNAPRO. Lithium hydroxide ($\geq 98\%$ pure, anhydrous, used as received from Sigma Aldrich, 1 mmol), nicotinic acid ($\geq 98\%$ pure, anhydrous, used as received from Sigma Aldrich, 1 mmol), and L-proline ($\geq 99\%$ pure, used as received from Sigma Aldrich, 2 mmol) were dissolved in 3.0 mL of deionized water and left to stand on a hot plate until block shape colorless crystals had emerged from solution.

Single-Crystal X-ray Data Collection and Structure Determinations. The X-ray diffraction data were collected using a Bruker-AXS SMART-APEXII CCD diffractometer (Cu K α , $\lambda = 1.54178$ Å). Indexing was performed using APEX2⁴¹ (Difference Vectors method). Data integration and reduction were performed using SaintPlus 6.01.⁴² Absorption correction was performed by multiscan method implemented in SADABS.⁴³ Space groups were determined using XPREP implemented in APEX2.⁴¹ The structure was solved using SHELXS-97 (direct methods) and refined using SHELXL-97 (full-matrix least-squares on F^2) contained in OLEX2⁴⁴ and WinGX v1.70.01^{45–48} programs.

LISPRO. All non-hydrogen atoms, except disordered C29a and C29b, were refined anisotropically. Hydrogen atoms of $-\text{CH}$, $-\text{CH}_2$, $-\text{NH}_2$, and $-\text{OH}$ groups were placed in geometrically calculated positions and included in the refinement process using riding model with isotropic thermal parameters: $\text{Uiso}(\text{H}) = 1.2\text{Ueq}(-\text{CH}, -\text{CH}_2, -\text{NH}_2)$, $\text{Uiso}(\text{H}) = 1.5\text{Ueq}(-\text{OH})$. One of the L-proline rings is disordered over two positions in a 1:1 ratio. SADI commands were used to restrain distances between disordered carbon atoms. The crystal was a twin, and refinement was conducted with an HKL5 type file generated using the $[-1/0/0; 0/-1/0; 0.14/0/1]$ twin law. This corresponds to 180° rotation about the $[001]$ reciprocal lattice direction. Crystallographic data is available in the Cambridge Structural Database

(CCDC 962323). The structure with probability ellipsoids is available in the Supporting Information (Figure S4).

LNAPRO. All non-hydrogen atoms were refined anisotropically. Hydrogen atoms of the $-\text{CH}$ and $-\text{CH}_2$ groups were placed in geometrically calculated positions and included in the refinement process using riding model with isotropic thermal parameters: $\text{Uiso}(\text{H}) = 1.2\text{Ueq}(-\text{CH}, -\text{CH}_2, -\text{NH}_2)$. Hydrogen atoms of the $-\text{NH}_2$ group were found from difference Fourier map inspection and were freely refined. Crystal data and refinement conditions are shown in Table 1. The L-proline ring

Table 1. Crystallographic Data and Structure Refinement Parameters

	LISPRO	LNAPRO
formula	$\text{C}_{12}\text{H}_{14}\text{LiNO}_5$	$\text{C}_{11}\text{H}_{13}\text{LiN}_2\text{O}_4$
MW	259.18	244.17
crystal system	monoclinic	orthorhombic
space group	$P2_1$	$P2_12_12$
a (Å)	10.3601(19)	10.2156(2)
b (Å)	10.1556(16)	10.4646(3)
c (Å)	12.173(3)	11.3811(3)
α (deg)	90.00	90.00
β (deg)	93.415(11)	90.00
γ (deg)	90.00	90.00
V (Å ³)	1278.5(4)	1216.66(5)
D_c (mg m ⁻³)	1.347	1.333
Z	4	4
2θ range	7.28–131.94°	7.76–131.9°
$N_{\text{ref}}/N_{\text{para}}$	6896/352	2116/183
T (K)	228(2)	228(2)
R_1 [$I > 2\sigma(I)$]	0.0394	0.0394
wR_2	0.0935	0.0935
GOF	0.988	0.988
abs coef.	0.872	0.843

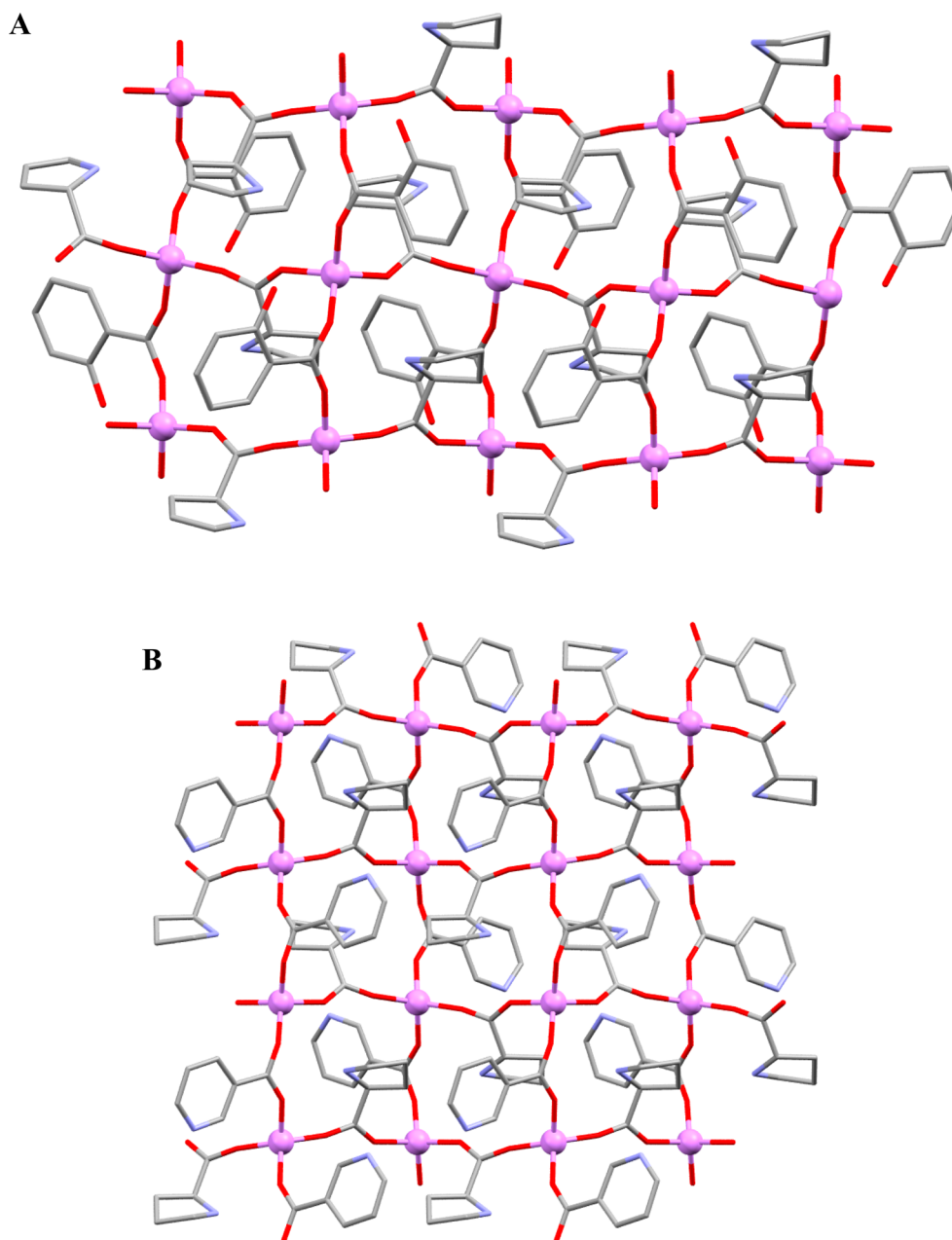


Figure 2. Crystal packing in LISPRO and LNAPRO. Square grid network exhibited by LISPRO (A) and LNAPRO (B). Hydrogen atoms are removed for clarity.

was found to be disordered over two positions with an approximate ratio of 0.7:0.3. Crystallographic data is available in the Cambridge Structural Database (CCDC 962324). The structure with probability ellipsoids is available in the Supporting Information (Figure S2).

Purity Confirmation. Powder X-ray diffraction (PXRD) and differential scanning calorimetry (DSC) were used to confirm the purity of the cocrystal preparations. PXRD patterns (from bulk samples) were compared to the calculated pattern (from the single crystal) and indicated that phase purity had been obtained (Figure 3). DSC indicated a clean single endotherm corresponding to the cocrystals. Prior to bioactivity and pharmacokinetics evaluation, purity was confirmed by preparing equimolar lithium solutions of LISPRO and LIS and measuring lithium concentration using atomic absorption spectrometry. The DSC (Figure S1) for LNAPRO is available in the Supporting

Information. The DSC (Figure S3) and AAS (Figure S5) data for LISPRO are available in the Supporting Information.

GSK-3 β Studies. Adult rat hippocampal neural stem cells (NSC, Millipore) were treated with LISPRO or LIS at 0, 1, and 5 mM for 40 h in a differentiation media. Cells were lysed using RIPA buffer with protease inhibitors cocktail and subjected to immunoblotting analysis using an antibody against phosphorylated phospho-GSK-3 β Ser9 (inactive form) or total GSK-3 β . Densitometry analysis was represented by ratio of phospho-GSK-3 β Ser9 to total GSK-3 β band intensity under WB from two independent experiments. *t*-tests were used to assess statistical significance in the ratio of phospho-GSK-3 β Ser9 to total GSK-3 β .

BDNF Studies. Mouse neuroblastoma (N2a) cells were grown in Dulbecco's modified Eagle's medium (DMEM) supplemented with 10% fetal bovine serum (FBS) and 1%

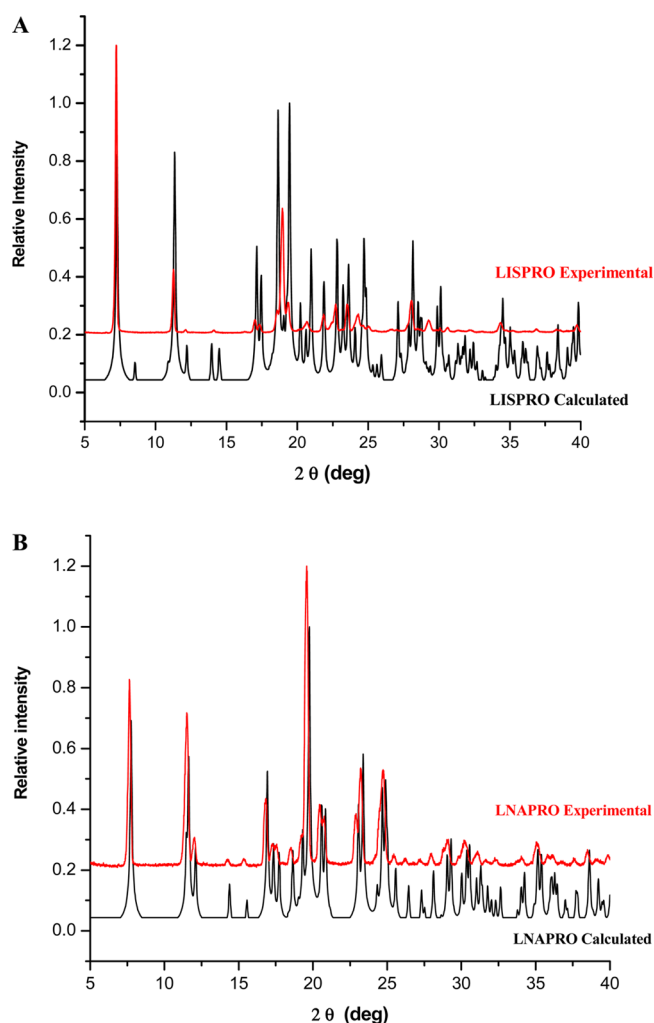


Figure 3. Powder X-ray diffraction patterns of LISPRO and LNAPRO. Experimental versus calculated PXRD of LISPRO (A) and LNAPRO (B).

penicillin-streptomycin. Cells were plated in 24-well plate at a density 5×10^4 cells per well in DMEM supplemented with 5% FBS and 1% penicillin-streptomycin. Twenty-four hours later, 1 and 10 mM of lithium as lithium salicylate (LIS) or cocrystal (LISPRO) were added to each well and incubated for 48 h. After treatment, media were collected for brain derived neurotrophic factor (BDNF) enzyme linked immunosorbent assay (ELISA) and cells were lysed for bicinchoninic acid assay (BCA). BDNF levels were measured in collected media with a BDNF Sandwich ELISA Kit (Millipore, cat. no. CYT306). Shortly, samples were incubated in a mouse anti-BDNF monoclonal antibody coated 96-well immunoassay plate at 4 °C, overnight on a shaker. The plates were thoroughly washed at least four times, and a biotinylated mouse anti-human BDNF monoclonal antibody was added to each well and incubated for 2.5 h at room temperature on a shaker. After washing, a streptavidin-enzyme conjugate solution was added and incubated at room temperature for 1 h on a shaker. After washing, a TMB/E substrate solution was added to the plates and inactivated after 7 min by adding the stop solution. The BDNF was detected immediately by measuring absorbance at 450 nm using a microplate reader. BDNF concentration was analyzed based on the BDNF standard curve and normalized to total protein concentration as determined using a BCA protein assay kit (Pierce, Rockford, IL).

LPS-Activated Microglia Studies. BV2 microglia cells were grown in DMEM supplemented with 10% FBS and 1% penicillin-streptomycin. Cells were plated in 24-well plate at a density 5×10^4 cells per well in DMEM with 10% FBS and 1% penicillin-streptomycin. Twenty-four hours later, 25 and 12.5 mM of lithium in DMEM as LIS or LISPRO were added to each wells and incubated for 30 min. The microglia were activated by the addition of 100 ng/mL or LPS. Six hours later, media was collected and NO was measured using a Griess Reagent system (Promega, Madison, WI) per the manufacturer's instructions.

Neuronal Differentiation Studies. Adult rat hippocampal neural stem cells were obtained from Millipore (Billerica, MA) and grown in expansion media that contained $1 \times B-27$ supplement minus vitamin A, 2 mM Gibco GlutaMAX, and 20 ng/mL bFGF in Neurobasal A medium (all from Gibco, Carlsbad, CA). After neurospheres formed, cells were plated on 12 mm poly-L-lysine coated coverslips (BD Biocoat, Bedford, MA) at density 5×10^4 cells/well in 3 mM LIS and LISPRO containing Neurobasal A medium only. Differentiation was induced for 5 days at 37 °C with 5% CO₂, and equal amounts of media was added to each well at day 3.

Immunocytochemistry. Cells were fixed with 4% paraformaldehyde (PFA, Sigma-Aldrich, St. Louis, MO) for 15 min at room temperature and washed with PBS for 5 min three times. Cells were then permeabilized with 1% Triton X-100 in PBS for 10 min at room temperature. After washing with PBS for 5 min three times, cells were blocked with 1% bovine serum albumin (BSA, Sigma-Aldrich, St. Louis, MO) in 0.02% Tween 20 containing PBS (PBST) for 10 min at room temperature with gentle shaking. Mouse monoclonal anti-Tuj1 (Covance, MMS 435P, 1:2000) and rabbit polyclonal anti-GFAP (Abcam, ab7260, 1:1000) antibodies were diluted in the blocking buffer and incubated for overnight at 4 °C with gentle shaking. After washing with 0.02% PBST 5 min for three times, goat anti-mouse Alexa Fluor 488 (1:250, green) and goat anti-rabbit Alexa Fluor conjugated 555 (1:250, red) (both from Abcam, Cambridge, MA) in blocking buffer were incubated for 45 min at room temperature. Nuclei were visualized by mounting with VECTASHEILD hardset mounting media with DAPI (Vector laboratory, Burlingame, CA). Fluorescence images were obtained by using a Zeiss microscope at 20× magnification. Scale bar = 20 μm.

Pharmacokinetics Studies. Male Sprague–Dawley rats weighing 200–250 g were purchased from Harlan. The animals were housed at the Moffitt Cancer Center vivarium (Tampa, FL) with a 12 h light–dark cycle. The rats were allowed to acclimate for a period of one week before any experiments are carried out. All experiments were conducted in accordance with USF IACUC approved protocols. They were allowed free access to food and water throughout the experiment. The rats were dosed via oral gavage with 4 mEq/kg elemental lithium as LISPRO or Li₂CO₃ dissolved in deionized water or suspended in 1% methylcellulose, respectively. Animals in each treatment group were euthanized at 2, 24, 48, and 72 h ($n = 3$ /time point), and blood was collected by cardiac puncture and carefully perfused with a pressure-controlled pump to maintain microvasculature integrity before removing brain tissue. Blood was centrifuged at 1600g at room temperature for 10 min, and plasma was separated. A 500 μL aliquot was diluted 10-fold in a 5% TCA and 10% IPA solution, vortexed, and allowed to sit for 10 min in order to precipitate proteins. These aliquots were centrifuged at 3000g for 30 min, and the supernatant was transferred to clean tubes prior to measuring lithium content using atomic absorption spectroscopy.

Table 2. LISPRO Hydrogen Bonds

D	H	A	$d(D-H)/\text{\AA}$	$d(H-A)/\text{\AA}$	$d(D-A)/\text{\AA}$	D-H-A/deg
N9	H9B	O3	0.91	1.84	2.750(6)	178.4
N11	H11A	O10 ^a	0.91	1.83	2.744(6)	176.6
N11	H11B	O7	0.91	2.01	2.873(8)	158.7
O26	H26	O4	0.83	1.92	2.640(9)	144.1
O28	H28	O5	0.83	1.82	2.557(7)	146.9

^a1 + X, +Y, +Z.

Table 3. LNAPRO Hydrogen Bonds

D	H	A	$d(D-H)/\text{\AA}$	$d(H-A)/\text{\AA}$	$d(D-A)/\text{\AA}$	D-H-A/deg
N5	H5A	O2	0.97(2)	1.83(2)	2.779(2)	163(2)
N5	H5B	O1 ^a	0.95(3)	1.81(3)	2.762(2)	176(2)

^a-1/2 - X, 1/2 + Y, -1 - Z.

(AAS). Brains were rinsed with PBS and weighed, and then an equal volume of concentrated HNO₃ was added. The brains were heated in this nitric acid solution for 1 h, allowed to cool to room temperature, and then centrifuged at 3000g for 1 h. The supernatant was removed and diluted 10-fold in 10% IPA prior to measuring lithium content using AAS (Shimadzu AA-6200). Peak height measurements were carried out referring to values obtained for standards of known concentrations. Lithium measurements are plotted as mean \pm SEM.

RESULTS

Crystal Structure Description. *Lithium Salicylate Proline, LISPRO.* Single crystal X-ray structural analysis reveals that LISPRO contains four lithium cations, four salicylate anions, and four L-proline molecules in the unit cell. There are two formula units in the asymmetric unit. Each lithium cation is linked to adjacent lithium cations by four bridging carboxylate moieties, two from salicylate and two from L-proline (Li-O distances: 1.916(1), 1.915(1) and 1.875(1), 1.905(1) Å). The overall network can be described as square grids and is illustrated in Figure 2A. The hydroxyl group of salicylate and protonated nitrogen of L-proline are involved in intramolecular and intermolecular hydrogen bonds (O-H...O⁻: 2.558(1) and 2.641(1); N⁺-H...O⁻: 2.751(1), 2.745(1) and 2.874(1) Å) (Table 2). The single crystal X-ray diffraction parameters of this and the other crystal structures reported herein are tabulated in Table 1.

Lithium Nicotinate Proline, LNAPRO. The crystal structure of LNAPRO reveals that the 1:1 ICC crystallized in space group *P*2₁2₁2 and that it contains four lithium cations, four nicotinate anions, and four L-proline molecules in the unit cell. There is one formula unit in the asymmetric unit. Two carboxylate moieties of nicotinate and two carboxylate moieties of proline molecules bridge adjacent lithium cations (Li-O distances: 1.897(3), 1.897(3) and 1.920(3), 2.920(3) Å). Undulating square grid networks are thereby generated as shown in Figure 2B. The protonated nitrogen atoms of proline form hydrogen bonds with carboxylate moieties (N⁺-H...O⁻: 2.779(2) and 2.762(2) Å) (Table 3).

LISPRO increases Phosphorylation of GSK-3 β in Rat Hippocampal Neural Stem Cells. Adult rat hippocampal neural stem cells (NSC, Millipore) were treated with LISPRO or LIS at 0, 1, and 5 mM for 40 h in a differentiation media and lysates subjected to immunoblotting analysis using an antibody against phosphorylated GSK-3 β Ser9 (phosph-GSK-3 β Ser9) or total GSK-3 β . The results from this experiment are shown in

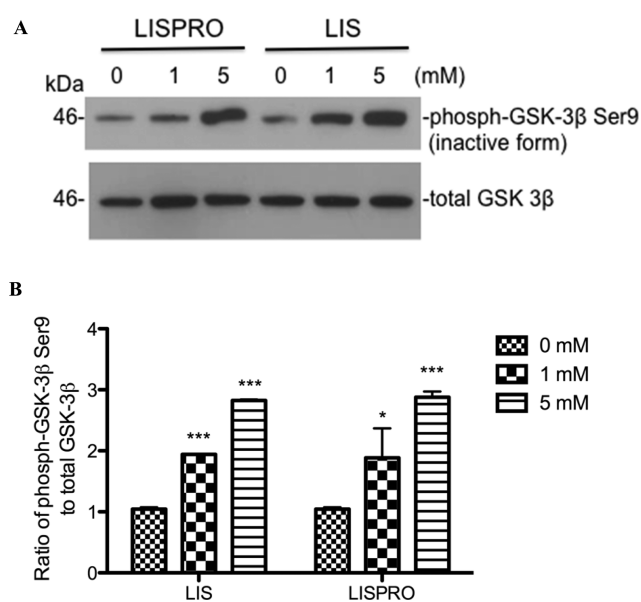


Figure 4. LISPRO treatment increases phosphorylation of GSK-3 β in adult rat hippocampal neural stem cells. Adult rat hippocampal neural stem cells (NSC, Millipore) were treated with LISPRO or LIS for 40 h in a differentiation media. (A) Cells were lysed by RIPA buffer with protease cocktails and subjected to immunoblotting (WB) analysis using an antibody against phosphorylated GSK-3 β Ser9 (phosph-GSK-3 β Ser9) or total GSK-3 β . (B) Densitometry analysis from two independent experiments is represented by ratio of phosph-GSK-3 β Ser9 to total GSK-3 β band intensity under WB. *t*-tests revealed significant differences in ratio of phosph-GSK-3 β Ser9 to total GSK-3 β for 1 and 5 mM of both LISPRO and LIS compared to control (**p* < 0.05, ****p* < 0.001). These results are representative of two independent experiments with *n* = 2 for each condition.

Figure 4. Densitometry analysis was represented by ratio of phosph-GSK-3 β Ser9 to total GSK-3 β band intensity under Western blot. The results of two independent experiments are shown in Figure 4B as mean \pm SEM. *t*-tests revealed significant differences in ratio of phosph-GSK-3 β Ser9 to total GSK-3 β in 1 and 5 mM of both LISPRO and LIS compared to control (**p* < 0.05, ****p* < 0.001). However, there were no significant differences in the ratio of LISPRO and LIS at equivalent concentrations, suggesting that ICCs of lithium remain bioactive and are bioequivalent to inorganic salts of lithium.

LISPRO Increases BDNF Production in Vitro. Mouse neuroblastoma (N2a) cells were treated with LIS and LISPRO at

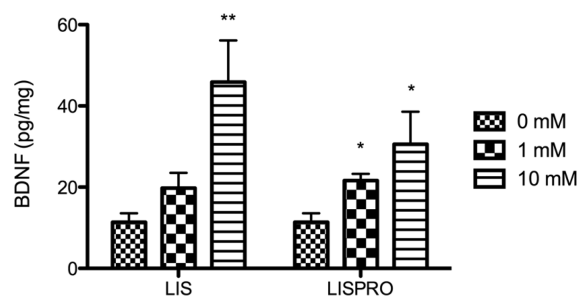


Figure 5. LISPRO treatment induces BDNF production by neurons. Neuroblastoma cells were treated with LIS and LISPRO for 48 h. BDNF was quantified in the media by ELISA and normalized to total protein in the cell lysate by BCA. *t*-tests revealed significant differences at 1 and 10 mM for LISPRO compared to the no treatment control ($*p < 0.05$) and only at 10 mM for LIS ($**p < 0.01$). There were no statistically significant differences between LIS and LISPRO at either concentration ($p > 0.05$).

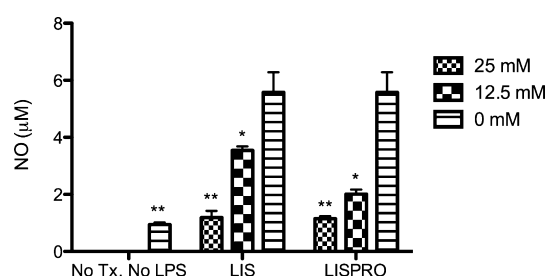


Figure 6. LISPRO treatment abolishes NO production in LPS-activated microglia. BV2 microglia were pretreated with LIS and LISPRO at 25 and 12.5 mM for 1 h prior to being activated by the addition of 100 ng/mL LPS. Eighteen hours later, media was collected and NO was measured. The no treatment, no LPS control group produced very low (basal) levels of NO. The no treatment with LPS control group produced the highest levels of NO. The lithium treatments abolished NO production at 25 mM and reduced it at 12.5 mM with LISPRO being advantageous at this concentration. Statistical significance from the no treatment with LPS control was assessed by *t*-tests ($*p < 0.05$, $**p < 0.01$, $***p < 0.001$).

5 and 25 mM in DMEM supplemented with 5% FBS for 48 h. BDNF quantification was determined via ELISA kit. We found that both LIS and LISPRO produced dose dependent increases in BDNF (Figure 5). This bioactivity of lithium has been previously reported for conventional lithium salts.^{10,49} This provides further evidence that the lithium remains bioactive despite being in the ICC form, LISPRO.

LISPRO Attenuates NO Production in LPS-Activated Microglia. BV2 microglia cells were treated with LIS and LISPRO at 12.5 and 25 mM in DMEM for 30 min prior to activation of microglia by 100 ng/mL LPS. NO was measured in the media 6 h later using a Griess Reagent system. Results are shown in Figure 6. We found that LPS increased NO production by BV2 microglia. Further, lithium treatment (both as LIS and LISPRO) attenuated this proinflammatory response. At 25 mM, both lithium forms completely inhibited NO production. At 12.5 mM, we found LISPRO to be more effective than LIS at attenuating NO production in these LPS-activated microglia. This supports the bioactivity of LISPRO and suggests that, in some instances, it may be advantageous to the parent salt form, LIS.

LISPRO Induces Neuronal Differentiation of Stem Cells.

Lithium has been shown to promote neuronal differentiation of hippocampal progenitor cells.⁵⁰ To test whether LISPRO possessed this bioactivity, we treated adult rat hippocampal neural stem cells with lithium as LIS and LISPRO at 3 mM for 5 days. Immunocytochemistry studies indicated that, compared to the no treatment control group (Figure 7A), both LIS (Figure 7B) and LISPRO (Figure 7C) did indeed promote differentiation of the progenitor cells into neurons over the course of the experiment.

LISPRO Pharmacokinetics in Rats. Male Sprague–Dawley rats weighing 200–250 g were dosed via oral gavage with 4 mEq/kg elemental lithium as the ICC LISPRO dissolved in deionized water or lithium carbonate (Li_2CO_3) suspended in 1% methylcellulose. Animals in each treatment group were euthanized at 2, 24, 48, and 72 h ($n = 3/\text{time point}$), and blood and brain were collected. Lithium was quantified using atomic absorption spectroscopy (AAS). Lithium measurements are plotted as mean \pm SEM in Figure 8. The plasma pharmacokinetics of Li_2CO_3 produced a sharp peak and rapid elimination with nearly undetectable levels at 48 h (Figure 8A). This produced a concomitant spike in brain lithium levels at 24 h (Figure 8B). LISPRO produced elevated lithium plasma levels at the earliest time point (2 h) (Figure 8C). The plasma lithium levels peaked at 24 h and remained elevated at 48 h before becoming almost undetectable at 72 h. LISPRO produced steady brain levels of lithium at 24 and 48 h (Figure 8D). The compilation of LISPRO versus Li_2CO_3 plasma (Figure 8E) and brain (Figure 8F) pharmacokinetics reveals some distinct differences between the ICC and salt forms. Although LISPRO produced very steady lithium plasma and brain levels out to 48 h, it was at the cost of bioavailability, which was clearly reduced compared to Li_2CO_3 in both the plasma and brain compart-

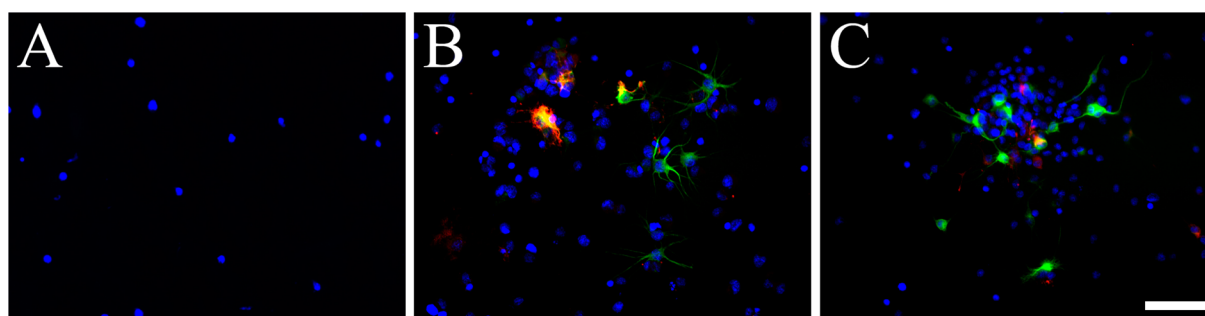


Figure 7. LISPRO induces neuronal differentiation of stem cells. Adult rat hippocampal neural stem cells were cultured with neurobasal media only (A), neurobasal media with 3 mM LIS (B), and neurobasal media with 3 mM LISPRO (C). Blue DAPI staining indicates nuclei, red GFAP staining indicates astrocytes, and green Tuj1 indicates neurons.

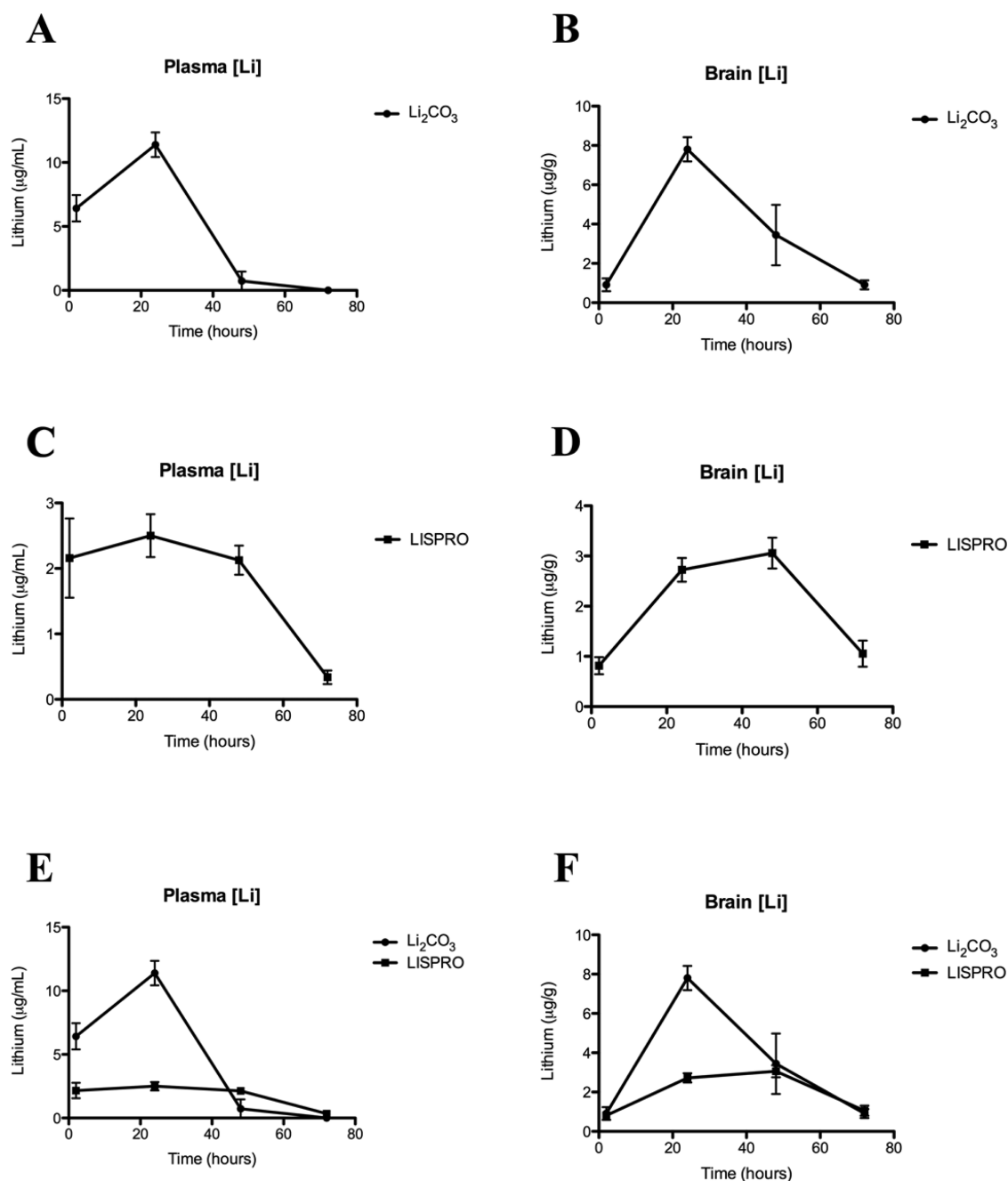


Figure 8. *In vivo* plasma and brain pharmacokinetics of LISPRO and Li₂CO₃. Male rats ($n = 3$ per formulation per time point) were dosed with 4 mEq/kg of lithium via oral gavage as LISPRO or Li₂CO₃. Plasma and brain lithium levels were determined at 2, 24, 48, and 72 h by atomic absorption spectrometry. (A) Li₂CO₃ plasma lithium concentration versus time (mean \pm SEM). (B) Li₂CO₃ brain lithium per gram of wet weight versus time (mean \pm SEM). (C) LISPRO plasma lithium concentration versus time (mean \pm SEM). (D) LISPRO brain lithium per gram of wet weight versus time (mean \pm SEM). (E) Compilation plasma lithium concentration versus time (mean \pm SEM). (F) Compilation brain lithium concentration versus time (mean \pm SEM).

ments. Relative plasma and brain bioavailability of LISPRO was 39% and 56%, respectively.

DISCUSSION

In regard to the therapeutic activity of various lithium salts for the treatment of bipolar disorder, equivalence is often assumed because the lithium cation is regarded as the API. Our bioactivity assessments of a new lithium ICC compared to the parent lithium salt supports this assumption only for the clinically relevant end points that we evaluated *in vitro*. Importantly,

because the molecular ideology of bipolar disorder is not fully understood, we cannot conclude that various forms of lithium will be equally effective at treating bipolar disorder *in vivo*. However, in this regard, we note that certain lithium salts alone might offer significant benefits from an efficacy and/or toxicity standpoint.

To our knowledge, there have been no side-by-side clinical evaluations of the therapeutic efficacy of the lithium salts that we utilized here. However, empirical evidence suggests that some of the anions might be therapeutically synergistic with lithium for the treatment of bipolar disorder. For example, a recent

pharmacoepidemiological study suggests that acetylsalicylic acid (aspirin) might be beneficial as an adjunct treatment with lithium salts for the treatment of bipolar disorder.⁵¹ The anion in LISPRO, salicylic acid, is the primary bioactive metabolite of aspirin. Stolk et al. reported that low-dose aspirin produced significant reduction in the relative risk of clinical deterioration in subjects on lithium and that this was not the case with other NSAIDs and glucocorticoids.⁵¹ The authors hypothesize that this is due to synergistic anti-inflammatory actions of lithium and acetylsalicylic acid by increasing the brain concentrations of 17-OH-DHA, an anti-inflammatory brain DHA metabolite. This hypothesis is supported by previous studies that demonstrated neuroinflammation in BD,⁵² that aspirin increases 17-OH-DHA,⁵³ and that lithium reduces neuroinflammation.^{54–56} Lithium nicotinate has been used in Russia for the treatment of alcoholism^{57–59} and stress.^{60,61} This lithium salt is distinguished by low toxicity and good tolerance.⁵⁸ Collectively, these findings suggest that lithium salicylate and lithium nicotinate might be advantageous to current FDA-approved lithium salts from efficacy and toxicity standpoints, respectively. As such, they are ideal as building blocks for the next generation of lithium therapeutics. Conversely, other lithium salts should probably be avoided for pharmaceutical applications. In two recent communications, Wouters et al. and Braga et al. reported new ICCs of lithium chloride and lithium bromide with racetams.^{36,38} Although racetams generally possess good toxicity profiles and might prove to act synergistically with lithium, bromide salts have been known to cause serious side effects that were coined bromism.^{62–64} This illustrates the importance of considering the safety of all components during crystal engineering studies that involve pharmaceutical materials. All components of LISPRO and LNAPO are considered pharmaceutically acceptable.

Development of multicomponent salt forms as APIs for the treatment of bipolar disorder would require high monetary investment and development of such drug products would therefore have to be enabled through exclusive intellectual property protection. Cocrystals of existing APIs have been deemed nonobvious and, therefore, patentable.³³ Moreover, they are known to modify the physicochemical properties and pharmacokinetics of an API. In our experiments, we synthesized and characterized novel ICCs of lithium salicylate and lithium nicotinate with the amino acid proline. LISPRO was selected for efficacy and pharmacokinetic evaluations due to the likelihood for additive or possibly even synergistic effects in treating neuropsychiatric diseases due to the biologically noninert anion, salicylic acid.

To our knowledge, this represents the first biological assessment of what is likely to become a very important class of pharmaceutical materials (ICCs). Our findings suggest that this change in speciation did not negatively affect the *in vitro* bioactivity of lithium at established targets for the treatment of neuropsychiatric disorders relative to the corresponding parent lithium salt. Furthermore, this is the first report of the pharmacokinetics of a cocrystal of a suspected BCS class I API as defined by Amidon et al.⁶⁵ Compared to an FDA-approved lithium salt, lithium carbonate (Li_2CO_3), in addition to being more efficacious by exploiting potential synergies, LISPRO may also offer a better safety profile due to unexpected pharmacokinetic changes. We found that a 4 mEq/kg dose of LISPRO to rats provided consistently elevated levels of lithium in the plasma and brain out to 48 h. Conversely, Li_2CO_3 was almost undetectable at 48 h in the plasma and produced a large spike in

the plasma and brain at 24 h post dose. This type of pharmacokinetic profile can contribute to the toxicity of lithium given its narrow therapeutic window. Indeed, Lippman and Evans suggested that an ideal lithium preparation would attenuate high blood level peaks and exhibit gradually declining blood concentrations.⁶⁶ This has been the driving logic behind the development and evaluation of many controlled release formulations.^{67–69} Recently, Emami et al. evaluated the pharmacokinetics of a proprietary sustained-release Li_2CO_3 formulation compared to Eskalith CR, the FDA approved controlled-release Li_2CO_3 formulation, and conventional Li_2CO_3 in man.⁶⁸ They found that the plasma spike produced by conventional lithium carbonate was greatly reduced in their proprietary formulation and Eskalith CR and conclude that this could be used to reduce the frequency of dosing and improve patient compliance. The pharmacokinetics exhibited by our ICC of lithium salicylate, LISPRO, is very similar to those in controlled release formulations. This apparent pharmacokinetic advantage of LISPRO compared to conventional lithium carbonate was unexpected. Although serendipitous in nature, this finding could be key in creating the next generation of lithium therapeutics. If these pharmacokinetic changes can be used to modify the dosing regimen for lithium therapy, this could improve patient compliance and reduce toxicity. Future studies are required to evaluate potential toxicity and efficacy advantages *in vivo* during maintenance lithium therapy conditions.

Since we have attained a more attractive *in vivo* pharmacokinetic profile and equivalent *in vitro* bioactivity at key therapeutic points, it would be quite significant if we could alleviate side effects *in vivo* or exploit synergistic activities with these or other lithium ICCs. Specifically, future studies are required to assess safety and efficacy advantages of lithium ICCs *in vivo*. Indeed, these findings represent an important initial step in the crystal engineering enabled development of the next generation of lithium therapeutics.

■ ASSOCIATED CONTENT

● Supporting Information

Additional data as described in the text. This material is available free of charge via the Internet at <http://pubs.acs.org>.

■ AUTHOR INFORMATION

Corresponding Author

*Phone: 813-974-1452. Fax: 813-974-3078. E-mail: asmith1@health.usf.edu.

Author Contributions

AS synthesized and characterized LISPRO, designed and conducted *in vivo* experiments, and wrote the paper. NKD synthesized and characterized LNAPO. LW solved the crystal structures. AS, JJ, and SK carried out *in vitro* experiments. JT, BG, and JE provided help and advice with *in vitro* experiments. RS and MZ managed the project and are joint senior authors. All authors contributed to final edits.

Notes

The authors declare the following competing financial interest(s): AS, ND, RS, and MZ are inventors on patent applications pertaining to these technologies.

■ ACKNOWLEDGMENTS

This work was supported by royalty research funds awarded to DS for the sublicense of a CNS drug. The authors would like to thank Margaret Baldwin, Todd Casagni, and Stacey Kubovec for

technical assistance during *in vivo* studies. The authors also thank Paula Bickford for graciously providing materials for the *in vitro* experiments.

■ ABBREVIATIONS LIST

API, active pharmaceutical ingredient; PXRD, powder X-ray diffraction; DSC, differential scanning calorimeter; FT-IR, infrared spectroscopy; TGA, thermogravimetric analysis; ICC, ionic cocrystal

■ REFERENCES

- (1) Shorter, E. The history of lithium therapy. *Bipolar Disord.* **2009**, *11* (Suppl 2), 4–9.
- (2) Thies-Flechtner, K.; Muller-Oerlinghausen, B.; Seibert, W.; Walther, A.; Greil, W. Effect of prophylactic treatment on suicide risk in patients with major affective disorders. Data from a randomized prospective trial. *Pharmacopsychiatry* **1996**, *29* (3), 103–107.
- (3) Goodwin, F. K.; Fireman, B.; Simon, G. E.; Hunkeler, E. M.; Lee, J.; Revicki, D. Suicide risk in bipolar disorder during treatment with lithium and divalproex. *JAMA* **2003**, *290* (11), 1467–1473.
- (4) Cipriani, A.; Hawton, K.; Stockton, S.; Geddes, J. R. Lithium in the prevention of suicide in mood disorders: updated systematic review and meta-analysis. *BMJ* **2013**, *346*, f3646.
- (5) Davenport, V. D. Distribution of parenterally administered lithium in plasma, brain and muscle of rats. *Am. J. Physiol.* **1950**, *163* (3), 633–641.
- (6) Ebadi, M. S.; Simmons, V. J.; Hendrickson, M. J.; Lacy, P. S. Pharmacokinetics of lithium and its regional distribution in rat brain. *Eur. J. Pharmacol.* **1974**, *27* (3), 324–329.
- (7) Livingstone, C.; Rampes, H. Lithium: a review of its metabolic adverse effects. *J. Psychopharmacol.* **2006**, *20* (3), 347–355.
- (8) Schou, M.; Baastrup, P. C.; Grof, P.; Weis, P.; Angst, J. Pharmacological and clinical problems of lithium prophylaxis. *Br. J. Psychiatry* **1970**, *116* (535), 615–619.
- (9) Fukumoto, T.; Morinobu, S.; Okamoto, Y.; Kagaya, A.; Yamawaki, S. Chronic lithium treatment increases the expression of brain-derived neurotrophic factor in the rat brain. *Psychopharmacology* **2001**, *158* (1), 100–106.
- (10) Leyhe, T.; Eschweiler, G. W.; Stransky, E.; Gasser, T.; Annas, P.; Basun, H.; Laske, C. Increase of BDNF serum concentration in lithium treated patients with early Alzheimer's disease. *J. Alzheimer's Dis.* **2009**, *16* (3), 649–656.
- (11) Yuskaitis, C. J.; Jope, R. S. Glycogen synthase kinase-3 regulates microglial migration, inflammation, and inflammation-induced neurotoxicity. *Cell. Signalling* **2009**, *21* (2), 264–273.
- (12) Frick, L. R.; Williams, K.; Pittenger, C. Microglial dysregulation in psychiatric disease. *Clin. Dev. Immunol.* **2013**, *2013*, 608654.
- (13) Ricken, R.; Adli, M.; Lange, C.; Krusche, E.; Stamm, T. J.; Gaus, S.; Koehler, S.; Nase, S.; Bschor, T.; Richter, C.; Steinacher, B.; Heinz, A.; Rapp, M. A.; Borgwardt, S.; Hellweg, R.; Lang, U. E. Brain-Derived Neurotrophic Factor Serum Concentrations in Acute Depressive Patients Increase During Lithium Augmentation of Antidepressants. *J. Clin. Psychopharmacol.* **2013**, *33* (6), 806–809.
- (14) Ghasemi, M.; Sadeghipour, H.; Mosleh, A.; Sadeghipour, H. R.; Mani, A. R.; Dehpour, A. R. Nitric oxide involvement in the antidepressant-like effects of acute lithium administration in the mouse forced swimming test. *Eur. Neuropsychopharmacol.* **2008**, *18* (5), 323–332.
- (15) Phiel, C. J.; Klein, P. S. Molecular targets of lithium action. *Annu. Rev. Pharmacol. Toxicol.* **2001**, *41*, 789–813.
- (16) Klein, P. S.; Melton, D. A. A molecular mechanism for the effect of lithium on development. *Proc. Natl. Acad. Sci. U.S.A.* **1996**, *93* (16), 8455–8459.
- (17) Alon, L. T.; Pietrovski, S.; Barkan, S.; Avrahami, L.; Kaidanovich-Beilin, O.; Woodgett, J. R.; Barnea, A.; Eldar-Finkelman, H. Selective loss of glycogen synthase kinase-3 α in birds reveals distinct roles for GSK-3 isozymes in tau phosphorylation. *FEBS Lett.* **2011**, *585* (8), 1158–1162.
- (18) Rowe, M. K.; Wiest, C.; Chuang, D. M. GSK-3 is a viable potential target for therapeutic intervention in bipolar disorder. *Neurosci. Biobehav. Rev.* **2007**, *31* (6), 920–931.
- (19) Yao, H. B.; Shaw, P. C.; Wong, C. C.; Wan, D. C. Expression of glycogen synthase kinase-3 isoforms in mouse tissues and their transcription in the brain. *J. Chem. Neuroanat.* **2002**, *23* (4), 291–297.
- (20) Avila, J.; Hernandez, F. GSK-3 inhibitors for Alzheimer's disease. *Expert Rev. Neurother.* **2007**, *7* (11), 1527–1533.
- (21) Dewhurst, S.; Maggirwar, S. B.; Schifitto, G.; Gendelman, H. E.; Gelbard, H. A. Glycogen synthase kinase 3 beta (GSK-3 beta) as a therapeutic target in neuroAIDS. *J. Neuroimmune Pharmacol.* **2007**, *2* (1), 93–96.
- (22) Yuskaitis, C. J.; Mines, M. A.; King, M. K.; Sweatt, J. D.; Miller, C. A.; Jope, R. S. Lithium ameliorates altered glycogen synthase kinase-3 and behavior in a mouse model of fragile X syndrome. *Biochem. Pharmacol.* **2010**, *79* (4), 632–646.
- (23) Allison, J. H.; Stewart, M. A. Reduced brain inositol in lithium-treated rats. *Nature (London), New Biol.* **1971**, *233* (43), 267–268.
- (24) Pollack, S. J.; Atack, J. R.; Knowles, M. R.; McAllister, G.; Ragan, C. I.; Baker, R.; Fletcher, S. R.; Iversen, L. L.; Broughton, H. B. Mechanism of inositol monophosphatase, the putative target of lithium therapy. *Proc. Natl. Acad. Sci. U.S.A.* **1994**, *91* (13), 5766–5770.
- (25) Harwood, A. J. Lithium and bipolar mood disorder: the inositol-depletion hypothesis revisited. *Mol. Psychiatry* **2005**, *10* (1), 117–126.
- (26) Singh, N.; Halliday, A. C.; Thomas, J. M.; Kuznetsova, O. V.; Baldwin, R.; Woon, E. C.; Aley, P. K.; Antoniadou, I.; Sharp, T.; Vasudevan, S. R.; Churchill, G. C. A safe lithium mimetic for bipolar disorder. *Nature Commun.* **2013**, *4*, 1332.
- (27) Goodwin, F. K.; Jamison, K. R. *Manic-depressive illness*; Oxford University Press: New York, 1990; pp xxi, 938.
- (28) Kilbane, E. J.; Gokbayrak, N. S.; Galynker, I.; Cohen, L.; Tross, S. A review of panic and suicide in bipolar disorder: does comorbidity increase risk? *J. Affective Disord.* **2009**, *115* (1–2), 1–10.
- (29) U.S. Food and Drug Administration. *Guidance for Industry: Regulatory Classification of Pharmaceutical Co-Crystals*; U.S. Food and Drug Administration: Silver Spring, MD, 2013.
- (30) Almarsson, O.; Zaworotko, M. J. Crystal engineering of the composition of pharmaceutical phases. Do pharmaceutical co-crystals represent a new path to improved medicines? *Chemical Commun.* **2004**, *17*, 1889–1896.
- (31) Desiraju, G. R. Supramolecular Synthons in Crystal Engineering—A New Organic Synthesis. *Angew. Chem.* **1995**, *34* (21), 2311–2327.
- (32) Moulton, B.; Zaworotko, M. J. From molecules to crystal engineering: supramolecular isomerism and polymorphism in network solids. *Chem. Rev.* **2001**, *101* (6), 1629–1658.
- (33) Almarsson, Ö.; Peterson, M. L.; Zaworotko, M. The A to Z of pharmaceutical cocrystals: a decade of fast-moving new science and patents. *Pharm. Pat. Anal.* **2012**, *1* (3), 313–327.
- (34) Smith, A. J.; Kavuru, P.; Wojtas, L.; Zaworotko, M. J.; Shytle, R. D. Cocrystals of quercetin with improved solubility and oral bioavailability. *Mol. Pharmaceutics* **2011**, *8* (5), 1867–1876.
- (35) Smith, A. J.; Kavuru, P.; Arora, K. K.; Kesani, S.; Tan, J.; Zaworotko, M. J.; Shytle, R. D. Crystal engineering of green tea epigallocatechin-3-gallate (EGCG) cocrystals and pharmacokinetic modulation in rats. *Mol. Pharmaceutics* **2013**, *10* (8), 2948–2961.
- (36) Wouters, J.; Grepioni, F.; Braga, D.; Kaminski, R. M.; Rome, S.; Aerts, L.; Quere, L. Novel Pharmaceutical Compositions through Co-crystallization of Racetams and Li⁺ Salts. *CrystEngComm* **2013**, *15*, 8898–8902.
- (37) Chierotti, M. R.; Gaglioti, K.; Gobetto, R.; Braga, D.; Grepioni, F.; Maini, L. From molecular crystals to salt co-crystals of barbituric acid via the carbonate ion and an improvement of the solid state properties. *CrystEngComm* **2013**, *15*, 7598–7605.
- (38) Braga, D.; Grepioni, F.; Maini, L.; Capucci, D.; Nanna, S.; Wouters, J.; Aerts, L.; Quere, L. Combining piracetam and lithium salts: ionic co-crystals and co-drugs? *Chem. Commun.* **2012**, *48* (66), 8219–8221.

- (39) Ong, T. T.; Kavuru, P.; Nguyen, T.; Cantwell, R.; Wojtas, L.; Zaworotko, M. J. 2:1 cocrystals of homochiral and achiral amino acid zwitterions with Li⁺ salts: water-stable zeolitic and diamondoid metal-organic materials. *J. Am. Chem. Soc.* **2011**, *133* (24), 9224–9227.
- (40) Braga, D.; Grepioni, F.; Maini, L.; Prosperi, S.; Gobetto, R.; Chierotti, M. R. From unexpected reactions to a new family of ionic cocrystals: the case of barbituric acid with alkali bromides and caesium iodide. *Chem. Commun.* **2010**, *46* (41), 7715–7.
- (41) Bruker APEX2, version 2008.1-0; Bruker AXS Inc.: Madison, WI, 2008.
- (42) SAINT, V6.28A; Data Reduction Software; Bruker AXS Inc.: Madison, WI, 2001.
- (43) Sheldrick, G. M. SADABS. Program for Empirical Absorption Correction; University of Göttingen: Göttingen, Germany, 1996.
- (44) Dolomanov, O. V.; Bourhis, L. J.; Gildea, R. J.; Howard, J. A. K.; Puschmann, H. OLEX2: A complete structure solution, refinement and analysis program. *J. Appl. Crystallogr.* **2009**, *42*, 339–341.
- (45) Farrugia, L. J. WinGX suite for small-molecule single-crystal crystallography. *J. Appl. Cryst.* **1999**, *32*, 837–838.
- (46) Sheldrick, G. M. SHELXL-97. Program for the Refinement of Crystal; University of Göttingen: Göttingen, Germany, 1997.
- (47) Sheldrick, G. M. A short history of SHELX. *Acta Crystallogr.* **2008**, *A64*, 112–122.
- (48) Sheldrick, G. M. Phase annealing in SHELX-90: Direct methods for larger structures. *Acta Crystallogr.* **1990**, *A46*, 467–473.
- (49) Rybakowski, J. K.; Suwalska, A.; Skibinska, M.; Dmitrzak-Weglarz, M.; Leszczynska-Rodziewicz, A.; Hauser, J. Response to lithium prophylaxis: interaction between serotonin transporter and BDNF genes. *Am. J. Med. Genet., Part B* **2007**, *144B* (6), 820–823.
- (50) Kim, J. S.; Chang, M. Y.; Yu, I. T.; Kim, J. H.; Lee, S. H.; Lee, Y. S.; Son, H. Lithium selectively increases neuronal differentiation of hippocampal neural progenitor cells both in vitro and in vivo. *J. Neurochem.* **2004**, *89* (2), 324–236.
- (51) Stolk, P.; Souverein, P. C.; Wilting, I.; Leufkens, H. G.; Klein, D. F.; Rapoport, S. I.; Heerdink, E. R. Is aspirin useful in patients on lithium? A pharmacoepidemiological study related to bipolar disorder. *Prostaglandins, Leukotrienes Essent. Fatty Acids* **2010**, *82* (1), 9–14.
- (52) Rao, J. S.; Harry, G. J.; Rapoport, S. I.; Kim, H. W. Increased excitotoxicity and neuroinflammatory markers in postmortem frontal cortex from bipolar disorder patients. *Mol. Psychiatry* **2010**, *15* (4), 384–392.
- (53) Serhan, C. N.; Hong, S.; Gronert, K.; Colgan, S. P.; Devchand, P. R.; Mirick, G.; Moussignac, R. L. Resolvins: a family of bioactive products of omega-3 fatty acid transformation circuits initiated by aspirin treatment that counter proinflammation signals. *J. Exp. Med.* **2002**, *196* (8), 1025–1037.
- (54) Basselin, M.; Kim, H. W.; Chen, M.; Ma, K.; Rapoport, S. I.; Murphy, R. C.; Farias, S. E. Lithium modifies brain arachidonic and docosahexaenoic metabolism in rat lipopolysaccharide model of neuroinflammation. *J. Lipid Res.* **2010**, *51* (5), 1049–1056.
- (55) Basselin, M.; Villacreses, N. E.; Lee, H. J.; Bell, J. M.; Rapoport, S. I. Chronic lithium administration attenuates up-regulated brain arachidonic acid metabolism in a rat model of neuroinflammation. *J. Neurochem.* **2007**, *102* (3), 761–772.
- (56) Yu, F.; Wang, Z.; Tchantchou, F.; Chiu, C. T.; Zhang, Y.; Chuang, D. M. Lithium ameliorates neurodegeneration, suppresses neuroinflammation, and improves behavioral performance in a mouse model of traumatic brain injury. *J. Neurotrauma* **2012**, *29* (2), 362–374.
- (57) Maksimovich, I. A.; Kresin, V. I.; Ariaev, V. L. Effectiveness of lithium nicotinate in the treatment of experimental alcoholism. *Byull. Eksp. Biol. Med.* **1983**, *96* (8), 35–37.
- (58) Kresyn, V. I.; Aryaev, V. L.; Kostev, F. I. Litonit: evaluation of clinical effectiveness. *Alcohol Alcohol.* **1993**, *28* (3), 333–337.
- (59) Kostev, F. I. Effect of Litonit and teturam on the course of biochemical processes in infectious inflammatory lesions of the kidneys in alcoholized animals. *Byull. Eksp. Biol. Med.* **1985**, *99* (6), 661–663.
- (60) Kresin, V. I. Stress-protective properties of lithium nicotinate—a new derivative of nicotinic acid. *Byull. Eksp. Biol. Med.* **1984**, *97* (3), 312–315.
- (61) Aksel'rod, L. B.; Kresin, V. I.; Moiseev, I. N.; Sukolovskaia, D. M.; Kravchenko, L. S. Functional changes in the myocardium and the reticular formation of the medulla oblongata in cardiogenic stress as affected by pharmacological correction with Litonit. *Byull. Eksp. Biol. Med.* **1988**, *105* (4), 453–455.
- (62) Kasteleijn-Nolstlt Trenite, D. G.; Edelbroek, P. M. Antiepileptic drug treatment in the nineties in The Netherlands. *Pharm. World Sci.* **1997**, *19* (2), 60–69.
- (63) Lugassy, D.; Nelson, L. Case files of the medical toxicology fellowship at the New York City poison control: bromism: forgotten, but not gone. *J. Med. Toxicol.* **2009**, *5* (3), 151–157.
- (64) Frances, C.; Hoizey, G.; Lamiable, D.; Millart, H.; Trenque, T. Bromism from daily over intake of bromide salt. *J. Toxicol., Clin. Toxicol.* **2003**, *41* (2), 181–183.
- (65) Amidon, G. L.; Lennernas, H.; Shah, V. P.; Crison, J. R. A theoretical basis for a biopharmaceutic drug classification: the correlation of in vitro drug product dissolution and in vivo bioavailability. *Pharm. Res.* **1995**, *12* (3), 413–420.
- (66) Lippmann, S.; Evans, R. A comparison of three types of lithium release preparations. *Hosp. Community Psychiatry* **1983**, *34* (2), 113–114.
- (67) Cooper, T. B.; Simpson, G. M.; Lee, J. H.; Bergner, P. E. Evaluation of a slow-release lithium carbonate formulation. *Am. J. Psychiatry* **1978**, *135* (8), 917–922.
- (68) Emami, J.; Tavakoli, N.; Movahedian, A. Formulation of sustained-release lithium carbonate matrix tablets: influence of hydrophilic materials on the release rate and in vitro-in vivo evaluation. *J. Pharm. Pharm. Sci.* **2004**, *7* (3), 338–344.
- (69) Ciftci, K.; Capan, Y.; Ozturk, O.; Hincal, A. A. Formulation and in vitro-in vivo evaluation of sustained-release lithium carbonate tablets. *Pharm. Res.* **1990**, *7* (4), 359–363.